A model based approach for identifying robust operating conditions for industrial chromatography with process variability

Edward J. Close [a,b], Jeffrey R. Salm [c], Daniel G. Bracewell [b], Eva Sorensen [a,*]

[a] Centre for Process Systems Engineering, Department of Chemical Engineering, University College London, Torrington Place, London WC1E 7JE, UK
[b] The Advanced Centre for Biochemical Engineering, Department of Biochemical Engineering, University College London, Torrington Place, London WC1E 7JE, UK
[c] Pfizer Biopharmaceuticals, 1 Burtt Road, Andover, Massachusetts 01810, USA

HIGHLIGHTS

- We consider a complex industrial bioseparation that experiences process variability.
- A mechanistic modeling approach is used to determine how to assure product quality.
- Probabilistic design spaces are generated from stochastic simulations.
- The impact of process parameter mean and variance on quality assurance is determined.
- Significant increases in robustness can be gained from adapting operating conditions.

ARTICLE INFO

ABSTRACT

A model based approach has been developed and used to identify robust operating conditions for an industrial hydrophobic interaction chromatography where resin lot variability, combined with feed stream variability, was resulting in serious performance issues during the purification of a multi component therapeutic protein from crude feed material. An equilibrium dispersive model was formulated which successfully predicted the key product critical quality attribute during validation studies. The model was then used to identify operating parameter ranges that assured product quality despite the process variability. Probabilistic design spaces were generated using stochastic simulations that showed the probability that each resin lot would meet product quality specifications, over a range of possible operating conditions, accounting for the historical variability experienced in the load material composition and concentration. No operating condition was found with normal process variability where quality assurance remained > 0.95 for resins that gave the highest and lowest product recoveries during process development. The lowest risk of batch failure found was 16%, and operating conditions were not robust. We then extended the stochastic methodology used to generate probabilistic design spaces, to identify the level of control required on the load material composition and concentration to bring process robustness to an acceptable level, which is not possible using DOE experimental methods due to the impractical amount of resources that would be required. Although reducing inlet variability resulted in an increase in the assurance of product quality, the results indicated that changing operating conditions according to which resin lot is in use is the favorable option.

1. Introduction

There is an increasing desire within the pharmaceutical industry to develop and operate processes following a Quality by Design (QbD) approach, where quality is built into the product and the process based on a high level of product knowledge and process understanding. In this approach, critical quality attributes (CQA) of pharmaceutical products are defined that assure desired clinical performance, and then a manufacturing process is designed to consistently meet these product attributes, thus assuring product quality (ICH, 2008a). Process characterization is conducted to identify the impact of process parameters on the products CQA's (Jiang et al., 2010), which is then used to define a process design space. A design space is defined by the International Conference on Harmonisation (ICH) guidance document as "the multidimensional combination and interaction of input variables and process

* Corresponding author.
E-mail address: e.sorensen@ucl.ac.uk (E. Sorensen).

parameters that have been demonstrated to provide an assurance of product quality" (ICH, 2008a). Acceptable ranges for process parameters and input variables are documented in the regulatory filing, and working within these ranges is not deemed to be a change from normal operating conditions. The expected benefit of the QbD approach is an increase in the assurance of product quality, and in turn, the FDA will allow manufacturers greater flexibility to operate with lower regulatory burden, enabling continuous process improvement, as well as greater robustness (ICH, 2005, 2008a, 2008b).

The current approach to process characterization to identify the design space, involves first performing a qualitative risk analysis to identify parameters for process characterization, e.g. failure mode effects analysis or fault tree analysis (ICH, 2005, Harms et al., 2008). Based on the outcome of this assessment, design of experiment (DOE) studies are conducted to generate data amenable for use in understanding and defining the acceptable parameter and input variable ranges that make up the design space (Rathore and Winkle, 2009). An important aspect of this characterization effort is concerned with validating that the defined design space can cope with the process variability experienced during normal operation (Rathore, 2009). This variability is a key driver in the current approach to the design and development of industrial biopharmaceutical separations, which promotes a focus on identifying the most robust operating conditions, rather than optimizing for particular scenarios. Process robustness is typically validated via an extensive experimental effort directed by factorial design of experiments to test that the product quality remains within the defined product attributes during normal operation, and this is approach is clearly suboptimal, time consuming and costly.

We consider an industrial chromatographic separation where resin lot variability, combined with a variable feed stream, had resulted in serious performance issues during the purification of a therapeutic protein from crude feed material. The resin lot variability occurred on a hydrophobic interaction chromatography (HIC) that provides impurity clearance whilst producing a complex product composed of six closely related variants of a *dimer* protein therapeutic ($\sim$30 kDa), with their *monomer* subunits in a specific ratio. Impurity removal is well understood; however, achieving the correct monomer subunit ratio poses a significant purification challenge. The desired ratio of monomer subunits must be met by this unit operation, and is a defined CQA of the final product. An extended range of resin lots were obtained from the supplier for testing within normal process operating ranges during process development conducted prior to this study. All resin lots were within the manufacturers specifications for ligand density and chloride capacity. Despite this, many failed to meet product quality specifications during testing and would have incurred significant losses if used for the large scale manufacture of the product. No link between resin lot specifications and successfully meeting process objectives was found.

Mechanistic models are ideally suited to assist in the development of robust purification processes, as they can efficiently investigate design alternatives with minimal experimentation, whilst deriving fundamental knowledge and process understanding in line with FDA recommendations. They have been successfully applied to many chromatographic separations (Melter et al., 2008; McCue et al., 2008; Nagrath et al., 2011), with useful examples on optimization (Degerman et al., 2007; Ng et al., 2012), scale up (Mollerup et al., 2007; Gerontas et al., 2010), and process development (Osberghaus et al., 2012), although the practical challenges of industrial separations mean their application to true industrial systems with crude feed mixtures is not yet routine, and can involve a lengthy experimental effort to calibrate parameters and validate predictions (e.g. Gétaz et al., 2013a,2013b; Nfor et al., 2013). Model based approaches to sensitivity and robustness analysis are of particular relevance to industrial separations as they can ensure purification processes are robust, which is a key requirement for bioseparations (Jakobsson et al., 2005; Degerman et al., 2009; Westerberg et al., 2012; Borg et al., 2013). These approaches enable the impact of disturbances in process parameters on meeting CQA's to be quantified quickly and efficiently, thereby indicating the risk of batch failure, with minimal time, material and analytical constraints. The additional knowledge and process understanding gained by their use may offset the extra investment of time and material for model development and validation, and fulfils regulatory guidance regarding the implementation of Quality by Design and the proposed greater use of mechanistic models (ICH, 2008a).

In this paper, a model based approach is developed and used to identify robust operating conditions for the HIC that ensure the desired product quality is met, despite the resin lot and inherent bioprocess variability. The HIC had predefined mobile phase conditions, flow rate and column dimensions that were fixed prior to this work, leaving the mass challenge and wash length as the only manipulated variables available for adjustment. An equilibrium dispersive model with competitive Langmuir adsorption is developed for the two most extreme resin lots which gave the highest (designated high binding resin) and lowest (designated low binding resin) protein recoveries at normal operating conditions. Micro well batch adsorption and scale down column experiments are used for model calibration, and the model is validated against multiple scale down column experiments over an extended range of inlet variables and process parameters.

The validated mechanistic model is then combined with stochastic simulation to generate probabilistic process design spaces for each resin lot. The results show the probability of meeting product quality specifications (i.e. product CQA's), over a range of possible operating conditions, whilst accounting for process uncertainty based on the historical variability experienced in the load material composition and concentration. The data is used to determine operating conditions that are eligible for all resin lots, by assuming that the operating conditions that assure product quality for the extreme high and low resin lots are suitable for all other resin lots. We then demonstrated how the stochastic methodology was used to generate probabilistic design spaces can be extended, when current uncertainty results in an unsatisfactory design space, in order to identify the level of control required on uncertain variables to bring process robustness to an acceptable level. The control required on the load material composition and concentration is determined. The presented approach can be used with any validated mechanistic model with parameters that are variable or uncertain, and enables the rapid exploration of the tradeoff between control of process parameters and the robustness of the design space, which is not possible using DOE experimental methods due to the impractical amount of resources that would be required.

FDA guidance encourages the application of mechanistic models to improve process understanding, based on fundamental knowledge of the underlying causes linking process parameters to product CQA's. The methodology demonstrates how useful mechanistic models can be for this task, for as well as determining the functional relationship between process parameter values and the resulting value of the CQA, the use of models can quickly and efficiently determine the relationship between process parameter and CQA variances, a key aspect of providing assurance of product quality.

2. Experimental materials and methods

2.1. Materials

2.1.1. Therapeutic protein and feed material

The product of interest is a disulfide linked dimer protein molecule (MW = 30 kDa), comprised of two monomer subunits. Three variations

of the monomer subunit exist due to slight variations in the amino acid sequence, here denoted A, $\bar{A}$ and B. This results in six possible isoforms of the dimer (AA, $A\bar{A}$, $\bar{A}\bar{A}$, $\bar{A}B$, AB and BB) as illustrated in Fig. 1. The corresponding analytical chromatogram is shown in Fig. 2A. Each form is an active component of the final product which must contain a specific ratio of the monomer subunits, $(A+\bar{A}):B$, i.e. not just one product form at a given total amount is required, but six closely related dimer variants, with a given ratio of their monomer subunits. Specifically, subunit B must account for between 25 and 45% of all monomer subunits in the product, i.e. $0.25 < B < 0.45$. In addition to the product, the HIC feed material contains several product related impurities accounting for up to 25% by mass of the feed material, including the individual monomer subunits (A, $\bar{A}$ and B), incorrectly formed product species (MW = 42, 60, 80 and 100 kDa), and host cell related contaminants consisting of mainly host cell protein (HCP) and DNA. The corresponding analytical chromatogram is shown in Fig. 2B.

2.1.2. Chromatography resin

Multiple (> 20) Butyl Sepharose 4B fast flow hydrophobic interaction resin lots were obtained from GE Healthcare (Uppsala, Sweden). The two most extreme resin lots were selected for this work based on protein recovery in process development experiments (not shown), and are designated high and low binding resin, e.g. the high binding resin gave high protein recoveries and the low binding resin gave low protein recoveries. Both resins were with the manufacturers' specifications.

2.1.3. Equipment

All preparative scale laboratory experiments were carried out using an ÄKTA FPLC chromatography system from GE Healthcare (Uppsala, Sweden). Laboratory columns were 1.1–3.2 cm in diameter and 7.4 cm in bed height. A GE Healthcare Mono S column (5.0 mm × 50 mm) high performance liquid chromatography (HPLC) column was used for analytics.
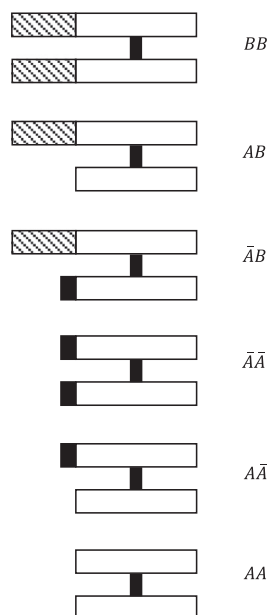
Fig. 1. The product is a disulfide linked dimer protein therapeutic (MW ≈ 30 kDa), comprised of two monomer subunits. Three variations of the monomer subunit exist due to slight variations in the amino acid sequence, here denoted A, $\bar{A}$ and B. This results in six possible forms of the dimer, all of which are active components of the final product and thus must be present in the elution peak in a specific distribution.
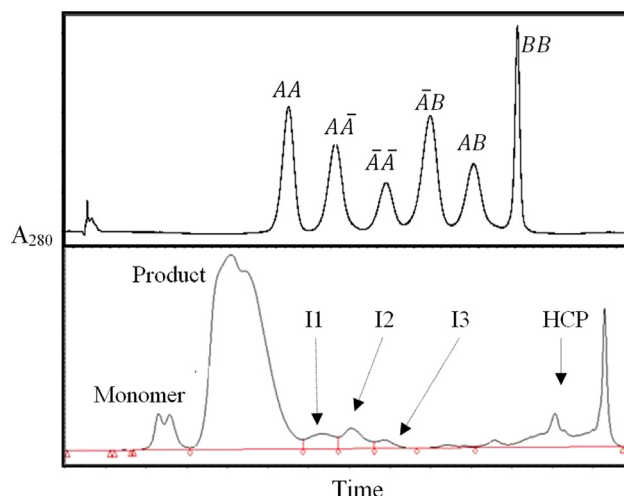
Fig. 2. Analytical chromatogram of Top. the product and Bottom. the feed material. (Axis values deliberately removed for confidentiality purposes).

2.2. Experimental methods

2.2.1. Hydrophobic interaction chromatography

During all runs, the columns were first equilibrated with 50 mM Tris, 1.0 M NaCl, 0.50 M Arg-HCl, pH 7 equilibration buffer. The elution peak from a preceding pseudo affinity capture chromatography was brought to the correct NaCl concentration and applied to the column at 4.2 CV/h, followed by a wash step using the equilibration buffer. Elution buffer consisting of 20% Propylene Glycol, 50 mM Tris, 0.50 M Arg-HCl, pH 7 was then applied and the product peak collected. The pooling policy was fixed for all runs. Any remaining bound protein was removed in a strip step using 0.1 M Sodium Acetate, pH 4 sanitization buffer, and the column was stored in storage buffer when not in use. The efficacy of the elution stage is well understood, and was experimentally validated during process development. Negligible amounts of protein remain in the column after the elution stage and all mass balances were satisfactory during experimental runs. All experiments were conducted between 4 and 8 °C.

2.2.2. Cation exchange HPLC assay

A cation Exchange (CEX) HPLC assay was used to determine the relative percentages of the six dimer isoforms of the product in samples, and utilized a Mono S column and a gradient of sodium acetate, acetonitrile and sodium chloride at pH 5. The relative percentage area of the six peaks in the chromatogram indicated the percentage of each isoform in the sample (Fig. 2. Top).

2.2.3. Phenyl reverse phase HPLC assay

A Phenyl Reversed Phase (RP) HPLC assay was used to determine the relative amount of product and product related impurities in samples, and utilized a TSK-Phenyl reversed phase column and a water/acetonitrile/trifluoroacetic acid gradient system (Fig. 2. Bottom).

2.2.4. Batch adsorption experiments

Batch adsorption experiments were required to generate data for calibrating the equilibrium adsorption isotherm parameters. Purified protein solutions for batch adsorption experiments were generated from bulk feed material by purifying and isolating product forms from impurities over multiple runs of the HIC. Batch binding studies based on the work of Coffman et al. (2008) were conducted in a 96-well filter plate and were repeated in triplicate. The filter plates used throughout the experiments were

round-well 800 μl plates with 0.45 μm pore-size polypropylene membrane. 25 μl of resin was taken from a bulk reservoir and dispensed by the robotic liquid handler into the individual wells as 25% (v/v) slurry in the appropriate equilibration buffer. The plate was then centrifuged to evacuate excess liquid and leave damp resin. Subsequently, other solutions composed of pure product, having various total protein concentrations (0.5–1 mg/ml) and isoform distributions (each component was varied between 20 and 60%) were added into wells containing the resin. The initial concentration and component distribution for each filter plate well were fashioned by mixing together protein from bulk solutions of known component distributions and concentrations, with the appropriate amount of equilibration buffer from a bulk solution in order that the total volume of liquid dispensed into each well was 275 μL (V_{tot}). The resin and solutions were then agitated on a platform shaker for 120 min. Separate batch uptake studies indicated that equilibrium was reached in less than 30 min (not shown), and therefore that this incubation time was suitable. Foil adhesive tape was used on the underside of the filter-plate to prevent liquid loss during shaking. After incubation, a centrifuge evacuated the supernatant into a UV-transparent 96 well micro plate which was stacked beneath the filter plate for analysis. The supernatant was then analyzed by a 96-well UV spectrophotometer (SpectraMax 250, Molecular Devices, Sunnyvale, CA) to determine the concentration of protein in the supernatant, C_i^m. CEX HPLC was used to determine the percentage of each component in the supernatant, P_i^m. The concentration of the protein in the mobile phase is calculated

$$C_i^m = \frac{C_{equil}P_i^m}{100} \qquad (1)$$

where C_i^m is the concentration of component i in the mobile phase (mg/ml), C_{equil} is the measured concentration in the supernatant of the micro well, determined by UV spectroscopy, and P_i^m is the percentage of component i in the mobile phase as determined by CEX HPLC. An elution cycle was then conducted following the same methodology as the load cycle, where 275 μL of elution buffer was added to each well, the plate agitated on a platform shaker for 120 min and the supernatant subsequently collected as described previously and analyzed using the spectrophotometer and CEX HPLC. The total amount of protein added to each micro well was then determined by Eq. (2)

$$M_t = \frac{C_{elution}}{V_{elution}} + \frac{C_{equil}}{V_{equil}} \qquad (2)$$

where M_t is the total amount of protein added to the microwell (mg), $C_{elution}$ is the concentration of the elution supernatant (mg/ml), $V_{elution}$ is the volume of the elution supernatant (ml), C_{equil} is the concentration of the equil supernatant (mg/ml), and V_{equil} is the volume of the equil supernatant (ml). The amount of protein adsorbed per unit volume settled resin, q_i (mg/ml), is calculated using Eq. 3:

$$q_i = \frac{\left(\frac{M_t P_i^{load}}{100} - C_i^m V_{equil} \right)}{V_{resin}} \qquad (3)$$

where P_i^{load} is the percentage of component i in the load material and V_{resin} is the settled volume of resin in the microwell (25 μl).

2.2.5. Pulse injection experiments

Pulse injection experiments were required to determine the total column porosity, ϵ_T. Pulses of NaCl were injected onto the column system and the retention time measured, accounting for dead time in the system. All experiments were performed in triplicate. The total column porosity, ϵ_T, was calculated by the following equation:

$$\epsilon_T = \frac{t_0 F}{V_C} \qquad (4)$$

where t_0 is the retention time of the unretained molecule (s), F is the mobile phase flowrate (ml/s), and V_C is the column volume (ml).

3. Mathematical methods

3.1. Process assumptions

The similar amino acid sequence of two of the monomer subunits (A and $\overline{A}$) results in similar separation properties of the product isoforms AA, $\overline{AA}$, $A\overline{A}$ and of the product isoforms $\overline{A}B$, AB. In order to simplify the modeling problem, the six product isotherms were reduced in the model to three components: AA, AB, and BB. We assumed that all product isoforms that remain bound to the column after the load and wash steps are subsequently collected in the elution step, thus only the load and wash stages of the separation are simulated, and that the product related impurities and HCP's in the feed stream had a negligible impact on the separation of the product of interest, as the impurities are observed to flow through during the load phase of the chromatographic cycle. Both of these assumptions were confirmed experimentally (Close et al., 2014).

3.2. Equilibrium dispersive model

An equilibrium dispersive model was chosen to simulate the HIC (Guiochon et al., 1994; Kaczmarski et al., 2001) as it is faster to solve than the general rate model, which was important for reducing total stochastic simulation time, and because fewer model parameters need to be determined, whilst still predicting the product CQA sufficiently well (as will be shown in Section 4). The model assumes that the mass transfer kinetics between the mobile phase moving through the column bed and the particles is infinitely fast. Thus the concentration of component i in the mobile phase is equal to the average concentration of component i in the intra-particular mobile phase, and the axial dispersion coefficient is replaced with an apparent axial dispersion coefficient, D_A (cm²/s), which includes the contribution from the mass transfer kinetics. The assumption was reasonable for this system due to the low flow rates (4.2 CV/h). The model has the following additional assumptions: (i) The column is unidimensional (radially homogeneous), (ii) the chromatographic separation is isothermal and adiabatic, (iii) the compressibility of the mobile phase is negligible and thus the velocity profile is flat, and (iv) the mass transfer parameters are independent of component concentration.

Assuming that the column is radially homogeneous, the differential mass balance in the bulk mobile phase is described by (Guiochon et al., 1994)

$$\frac{\partial C_i^m}{\partial t} + \frac{(1-\epsilon_T)}{\epsilon_T}\frac{\partial C_i^{sp}}{\partial t} + u\frac{\partial C_i^m}{\partial z} = D_A\frac{\partial^2 C_i^m}{\partial z^2} \quad \forall i = 1, 2, \ldots, N_C \quad z \in (0, L) \qquad (5)$$

where C_i^m is the concentration of component i in the mobile phase (mg/ml), t is the time (s), ϵ_T is the total column porosity, C_i^{sp} is the concentration of component i in the stationary phase (mg/ml), u is the interstitial velocity (cm/s), z is the axial coordinate, D_A is the apparent axial dispersion coefficient (cm²/s), N_C is the number of components in the system, and L is the column length (cm). $\partial C_i^m/\partial t$ is the rate per unit volume of accumulation of component i in the mobile phase, $((1-\epsilon_T)/\epsilon_T)(\partial C_i^{sp}/\partial t)$ is the rate per unit volume of accumulation of component i in the stationary phase,

$u(\partial C_i^m/\partial z)$ is the rate per unit volume of mass transfer by convection down the column, and $D_A(\partial^2 C_i^m/\partial z^2)$ is the rate per unit volume of mass transfer by dispersion and particle mass transfer kinetics lumped into one term.

The boundary conditions for Eq. (5) are the following:

At the inlet of the column, $z=0$, the mobile phase concentration, C_i^m, depends on convection and dispersion:

$$\left[uC_i^m - D_A\frac{\partial C_i^m}{\partial z}\right]\Bigg|_{z=0} = uC_{i,0}^m \qquad i=1, 2, \ldots, N_C \tag{6}$$

where $C_{i,0}^m$ is the inlet concentration.

At the outlet of the column, $z=L$, only convective transport is considered:

$$\frac{\partial C_i^m}{\partial z}\Bigg|_{z=L} = 0 \qquad \forall i=1, 2, \ldots, N_C \tag{7}$$

An initial condition is also required to solve Eq. (5), and this states that the rate per unit volume of accumulation in the mobile phase of component i within the column at $t=0$ is zero:

$$\frac{\partial C_i^m}{\partial t} = 0 \quad 0 < z < L \qquad \forall i=1, 2, \ldots, N_C \tag{8}$$

Protein adsorption onto the stationary phase was modeled using a competitive Langmuir adsorption isotherm (Seidel-Morgenstern, 2004).

$$q_i = \frac{q_s k_{a,i} C_i^m}{1+\Sigma k_{a,i} C_i^m} \qquad \forall i=1, 2, \ldots, N_C \qquad z \in (0,L) \tag{9}$$

where q_s is the resin saturation capacity, and $k_{a,i}$ is the equilibrium constant of component i, and q_i represents the amount of protein adsorbed per unit volume of settled resin. When the adsorption isotherm (Eq. 9) is linked with the differential mass balance in the bulk mobile phase (Eq. 5), the amount of protein adsorbed per unit volume of *settled resin*, q_i, is converted to the amount of protein adsorbed per unit volume of *stationary phase* in the packed bed, C_i^{sp}:

$$C_i^{sp} = \frac{CFq_i}{(1-\epsilon_T)} \qquad \forall i=1, 2, \ldots, N_C \qquad z \in (0,L) \tag{10}$$

Where, dividing q_i by $(1-\epsilon_T)$ accounts for the phase ratio (Mollerup, 2008), and multiplying q_i by a compression factor, CF, defined as the ratio between settled bed volume and packed bed volume, accounts for bed compression (Gerontas et al., 2010). The necessary compression had been determined experimentally during process development in order to prevent the formation of column headspace under flow conditions. All model equations are implemented and solved using the dynamic simulation tool gPROMS™ (Process Systems Enterprise, 2013). Discretization of the column in the axial coordinate is done using the built-in orthogonal collocation on finite element method (OCFEM).

3.3. Parameter estimation

The 'parameter estimation' entity in gPROMS™ is based on the SRQPD sequential quadratic programming code and was used to fit adsorption isotherm parameters in Eq. (9) (q_s, $k_{a,i}$) and the apparent axial dispersion coefficient in Eq. (5) (D_A). Parameter estimation was based on the maximum likelihood formulation, which determines values for the uncertain physical and variance model parameters that maximize the probability that the model will predict measured values from development experiments (Process Systems Enterprise, 2013). First the adsorption isotherm parameters are estimated by fitting the competitive Langmuir isotherm model to the three component competitive adsorption data from the micro well batch adsorption experiments (Section 2.2.4). For estimation of the apparent axial dispersion

coefficient, the full equilibrium dispersive model with competitive Langmuir adsorption is fitted to experimental product form distributions in samples taken every CV during the wash of a scale down column run (Section 2.2.1.).

3.4. Stochastic simulations

The sequence of calculations is illustrated in an example shown in Fig. 3, which is discussed in detail in the results and discussion section of this work. For variables of interest, instead of assigning a literal value, a stochastic value is assigned where the batch to batch variability is accounted for by specifying the average and standard deviation. When simulating the chromatography using the model, a built in function within gPROMS is used that returns a random value sampled from a normal distribution generated using the specified average and standard deviation. Each time a simulation is run, a different value is picked for the variable of interest. Multiple simulations (>5000) were conducted at each unique operating point in order to determine how variability in the variable of interest affects the ability of the process to meet critical quality attributes (CQA) of the outlet stream, as defined by the process objectives. The CQA considered was the ratio of the monomer subunits, $(A+\overline{A}):B$ in the elution pool. In each individual simulation, the variable of interest is randomly assigned at the start of the simulation and the resulting CQA is recorded at the end and used to generate a probability density function (PDF). By normalizing the PDF by the total number of simulations, the area under the PDF curve is equal to one, therefore, the area under the curve where the process objective is met is the probability that the objective will be met at that operating point. The probability of meeting the process objective is calculated for all potential operating points and combined into one graph to generate a probabilistic design space which shows the probability of meeting the process objective at each operating point, considering process variability.

In this work, we considered the variability in the load material concentration and composition, and neglected the impact of errors in model predictions, as well as uncertainty in controlled variables such as ionic strength, bed height etc. Our rational for this is discussed later. The exact parameter varied in the mechanistic model was the inlet concentrations of the load material, $C_{i,0}^m$. Historical averages and standard deviations from manufacturing data were used to generate probabilistic design spaces for current process variability (Table 1). In order to identify the level of control required on uncertain variables to bring process robustness to an acceptable level when current uncertainty results in an unsatisfactory design space, standard deviations in model simulations were manually assigned assuming that better control would result in less variability, and therefore a reduced standard deviation. Manually changing the load concentration average is also possible, and may be of interest as feed dilution is trivial, but this was not considered in this work.

Simulation time for each operating point was approximately 20 minutes using a 3.4 GHz AMD Phenom II X4 965 processor with 8 GB DDR3 RAM. A multi scale model was formulated within gPROMS and linked with Excel enabling all simulations (i.e. calculations at all operating points) to be conducted overnight, with data automatically exported to Microsoft Excel and transformed into probabilistic design spaces.

4. Results and discussion

4.1. Model calibration

Targeted micro well batch adsorption experimentation (Section 2.2.4.) was utilized to generate data for estimating the
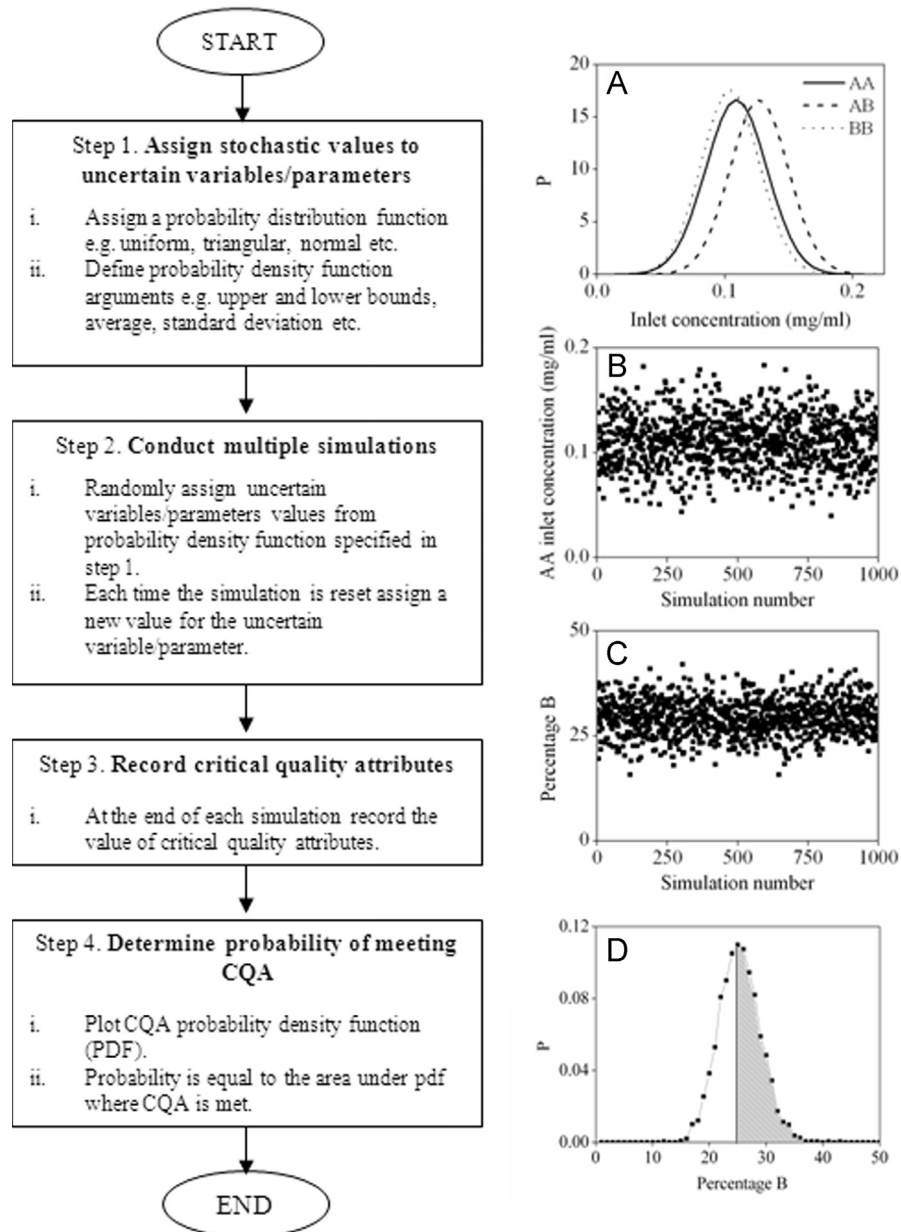
Fig. 3. Example of the stochastic modeling technique used in this work. (A) Normal distribution of inlet concentration of example product form from historical operating data. (B) Example of randomly selected inlet concentrations of product form *AA* during the first 1000 stochastic simulations. (C) Percentage *B* in elution peak over the first 1000 simulations. (Mass challenge 2 mg/ml, 5 CV wash length). (D) Probability density function of product CQA (%B) with area highlighted where product quality is met.

Table 1
Historical average and standard deviations of product form inlet concentrations.

Variable name	Variable notation	Average (mg/ml)	Standard deviation
AA inlet concentration	$C_{1,0}^m$	0.108	0.024
AB inlet concentration	$C_{2,0}^m$	0.127	0.023
BB inlet concentration	$C_{3,0}^m$	0.104	0.023

adsorption isotherm parameters, q_s, $k_{a,i}$. Fig. 4 shows the multi-component competitive adsorption data from the micro well experiments for the high and low binding resin lots, at four different load material product distributions shown on the graphs in the ratio *AA%:AB%:BB%*. The product form distribution in the load material was varied to ensure that the competition between the closely related product forms was captured in the isotherm model. Note that although the graphs show the bound concentration, q_i, of the product form as a function of its mobile phase concentration, C_i, the mobile phase concentration of the other two product forms are also affecting the bound concentration.

The estimated isotherm parameter values are shown in Table 2. The standard deviations of the estimated parameters are approximately ten percent, indicating there is still some uncertainty in the parameter values. The coefficient of determination, r^2, for the model fit to experimental data was 0.93 for the high resin and 0.96 for the low resin. This was found to be sufficient for satisfactory agreement between model predictions and experimental data given the inherent uncertainties of the batch adsorption experiments (Seidel-Morgenstern, 2004). Interestingly, the estimated saturation capacity of the Langmuir isotherm, q_s, were similar for both resins; however, the equilibrium constants differed for all three components. This indicated that the source of the resin lot variability was associated with protein adsorption-desorption kinetics and not the maximum saturation capacity. A detailed investigation into the exact mechanism behind this variability was beyond the scope of this work, but would be of great interest.

Both resin lots showed significant competition between product forms, with component BB particularly vulnerable to displacement by the more strongly binding AA and AB forms. In graph 4C, the BB stationary phase concentrations are significantly higher compared to Graph 4B. This is due to the favorable product distribution in the load material resulting in fewer competing components, allowing more BB to bind (graph 4C load material 20% AA:25% AB:55% BB, graph 4B load material 28% AA:59% AB:13% BB). It was found that the low binding resin had lower binding capacities than the high binding resin. This was especially clear for the BB component as shown in Fig. 4C where the low binding resin BB stationary phase concentration is approximately half that of the high binding resin.

Pulse injections onto scale down columns (Section 2.2.5) using an unretained molecule (NaCl) found that both resin lots had the same total column porosity, ($\epsilon_T = 0.9 \pm 0.02$), which was in agreement with the previous literature estimations for this resin (McCue et al., 2007).

The apparent axial dispersion coefficient, D_A, was estimated by fitting the full equilibrium dispersive model to experimental product form distributions in samples taken every CV during the wash of a scale down column run. We found that the estimated apparent axial dispersion coefficients, D_A, for high and low binding resin lots were very similar (high resin=0.029 cm^2/s and low

resin=0.03 cm^2/s), indicating that mass transfer was not responsible for differences between the resin lots.

4.2. Model validation

Multiple scale down column runs were conducted for each resin lot in order to provide a rigorous test of model predictive capacity, where the product form distribution was measured across the wash phase and in the elution peak. An extensive experimental validation of model predictive capability across the complete design space to be explored was unfeasible due to industrial time and material constraints. However, the isoform distribution in the load material, total load concentration and load challenge were carefully selected (Table 3) to provide wide ranging coverage of the envisaged design space, and model predictions were also compared with existing elution peak product data from scale down experiments which had been conducted previously by Pfizer purification process development, at load concentrations, load challenges and wash lengths considerably different from those conducted by the authors of this work. The flowrate, F, wash length, t, bed compression, and bed height, L, were kept constant throughout all runs (compression factor for both resins=1.25), and a range of column volumes were used (7, 15 and 60 ml). For both resins, the model was able to

Table 2
Model parameter values obtained for low and high binding resins based on batch adsorption and scale down column experiments, fitted using parameter estimation in gPROMS.

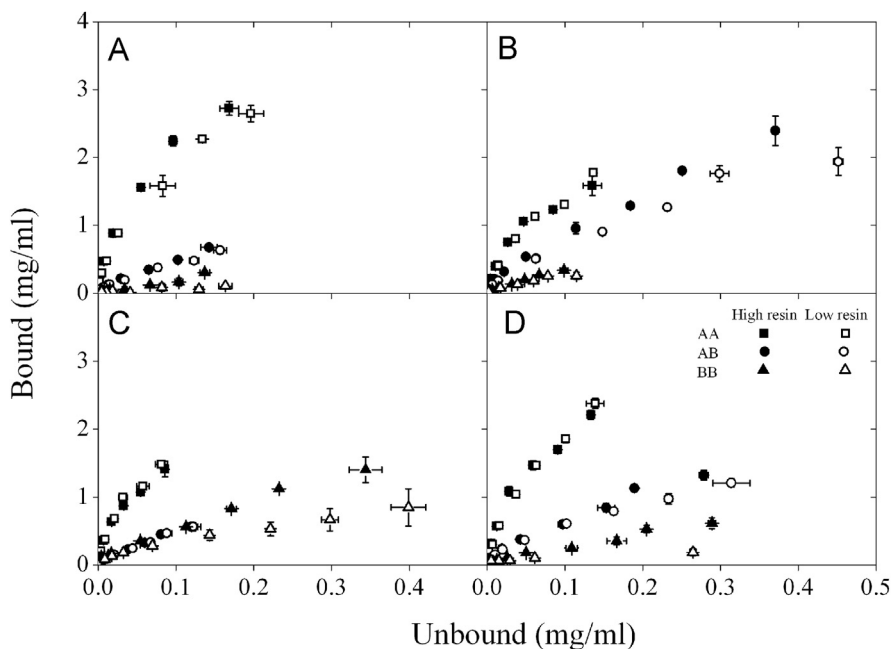| Parameter name	Parameter notation	Low	High
AA equilibrium constant	$k_{a,1}$	4.33	6.33
AB equilibrium constant	$k_{a,2}$	1.49	2.30
BB equilibrium constant	$k_{a,3}$	0.52	1.01
Saturation capacity (mg/ml)	q_s	6.45	6.39
Total column porosity	ϵ_T	0.9	0.89
Apparent axial dispersion coefficient (cm^2/s)	D_A	0.0029	0.003

Fig. 4. Multi-component competitive adsorption isotherms for the high and low binding resin lots, at a range of load material product distributions as shown on the graphs in the order AA%: AB%: BB%. (All experimental points were repeated in triplicate and standard error is shown on the graphs). (A) 53:26:21, (B) 28:39:13, (C) 25:20:55 and (D) 31:37:32.

successfully predict the product form distribution across the wash and in elution peaks in all scale down model validation column runs, both from this work, and those conducted separately by Pfizer. Fig. 5 shows examples where model predictions are compared with experiments. Model elution peak composition was consistently within ± 5% of experimentally measured values (values reported in Table 4), which was similar to the accuracy seen in design of experiment driven statistical response surface models of this process at Pfizer. This is significant, as it demonstrates that despite the complex feed stream and wide range of conditions tested, a relatively simplistic equilibrium dispersive model can provide similar accuracy predictions to a DOE type approach to design space generation, often used in industry.

4.3. Stochastic simulations

The mechanistic models developed for the high and low resin lots can determine the operating conditions where product quality specifications will be met for a known inlet concentration and composition. However, in practice, for industrial chromatographic separations the feed material is often uncharacterised prior to column loading, and will vary from batch to batch depending on upstream operations. In this work, a model based approach combining the validated mechanistic model with stochastic simulation is used to account for the inherent variability of inlet concentration and composition when determining the ability of a resin lot to meet the process objectives (or conversely the risk of batch failure).

The methodology is illustrated in an example which shows the data generated at one potential mass challenge – wash length combination. The component inlet concentration distributions were generated from historical data, and are shown in Fig. 3A. Averages and standard deviations are shown in Table 1. For

illustrative purposes the first 1000 randomly generated inlet concentrations of product form AA is shown in Fig. 3B, and the corresponding value of the product CQA (i.e. subunit B must account for between 25 and 45% of all monomer subunits in the product, i.e. $0.25 < B < 0.45$) is shown in Fig. 3C. It is a straightforward procedure to generate useful statistical information with this data regarding CQA variance at each operating point, such as moments and quartiles, as shown in Fig. 6 for the low binding resin. The statistical data can be conveniently displayed using a box and whisker plot. The bottom and top of the box are the first and third quartiles, and the band inside the box is the median. The end of the lower whisker represents the datum still within 1.5 interquartile range (IQR) of the lower quartile, and the end of the upper whisker represents the datum still within 1.5 IQR of the upper quartile. The minimum and maximum of the data is indicated in the whiskers by a straight line, and the 1% and 99% quartiles are represented by crosses. Outliers are plotted as dots. More sophisticated statistical techniques can be employed to analyze multivariate interactions and CQA dependencies. The derived data can play a key role in the quality risk assessments recommended by FDA guidance when developing quality products (ICH, 2005). The data was transformed into probability density functions which were used to calculate the probability of meeting the product CQA as a function of inlet uncertainty, as also shown in Fig. 6. Probabilistic design spaces were then generated by plotting the probability of meeting the product CQA (B%) as a function of available manipulated variables, e.g. mass challenge and wash length.

Table 3
Model validation runs: product percentage in load, load concentration, and load challenge.

Run identifier	Load Challenge (mg/ml resin)	Load Concentration (mg/ml)	AA %	AB %	BB %
A	1.5	0.26	35	35	30
B	2.2	0.35	40	44	16
C	2.4	0.44	14	38	48

Table 4
Model validation runs: Experimental vs simulated percentage A and B in elution peaks.

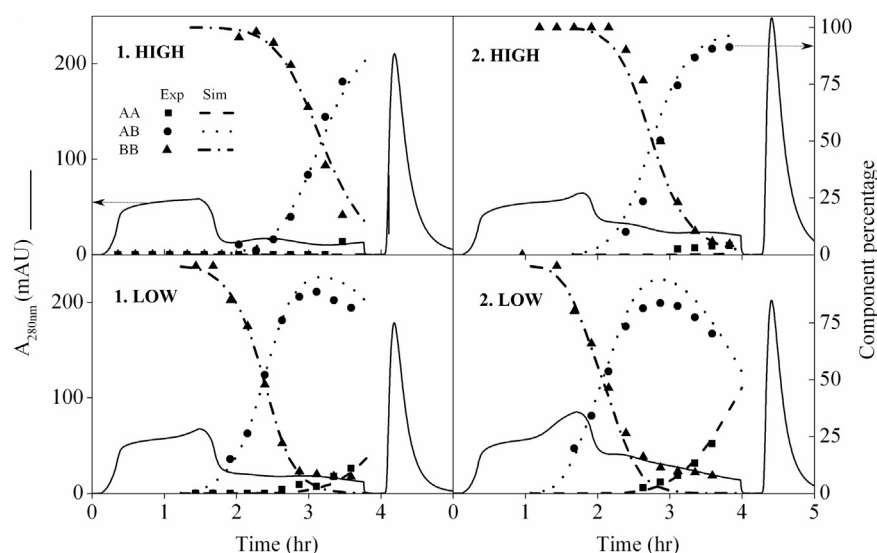| Resin identifier	Run identifier	Exp % A	Sim % A	Difference	Exp % B	Sim % B	Difference
High	A	81	79	− 3	19	21	+ 3
	B	85	82	− 3	15	18	+ 3
	C	71	68	− 3	29	32	+ 3
Low	A	90	90	0	10	10	0
	B	93	93	0	7	7	0
	C	86	81	− 5	14	19	+ 5

Fig. 5. Experimental and simulated product form distributions during load, wash and in final elution peak in model validation runs. Top. High resin. Bottom. Low resin. Left. Case study A. Right. Case study B. (7 ml CV, 7.4 cm bed height, 4.2 CV/h, load details shown in Table 3).
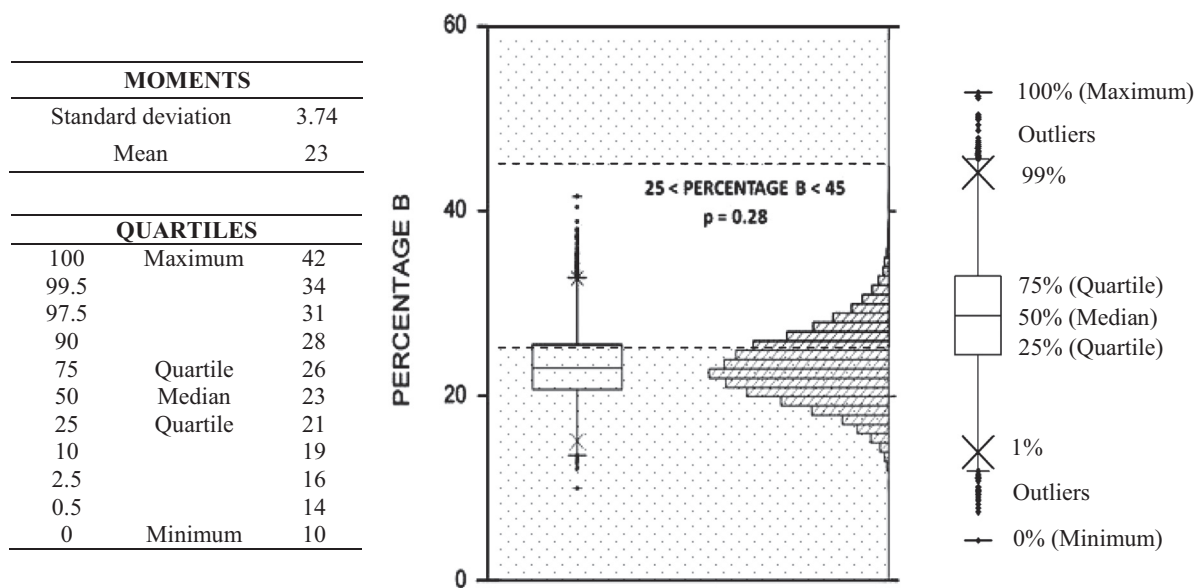
MOMENTS		
Standard deviation		3.74
Mean		23

QUARTILES		
100	Maximum	42
99.5		34
97.5		31
90		28
75	Quartile	26
50	Median	23
25	Quartile	21
10		19
2.5		16
0.5		14
0	Minimum	10

Fig. 6. CQA data from stochastic simulation at mass challenge 2.5 mg/ml, wash length 5 CV in box plot and probability distribution form with associated moments and quartiles (low resin).
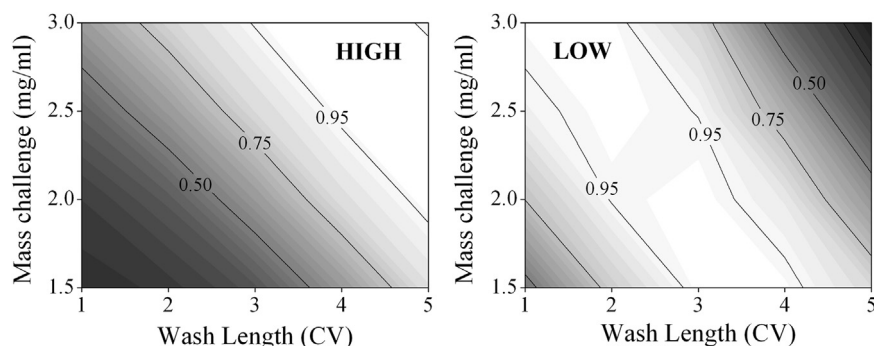

Fig. 7. Probabilistic design spaces for low binding (right) and high binding (left) resin lots, showing the probability that the resin will achieve the correct product form distribution in the elution peak over a ranges of possible mass challenges and wash lengths.

Accounting for uncertainty in controlled variables such as ionic strength was beyond the scope of this work, but can be integrated into simulations if desired. In this case, a suitable isotherm with a parameter that can be assigned uncertainty concerning ionic strength, such as the steric mass action (SMA) isotherm, would be required (Brooks and Cramer, 1992). In addition, the impact of model uncertainty on stochastic predictions can be included, although this was neglected in this work as the CQA variance (e.g. 10–42% in the example shown in Fig. 6) was typically much larger than the largest model error found during model validation studies ($\pm 5\%$). Despite this, the uncertainty in model predictions cannot be easily neglected and care must be taken to ensure that robust operating areas identified by model predictions are tested experimentally.

Probabilistic design spaces for the low and high resin lots are shown in Fig. 7. The design space is defined as the multidimensional combination and interaction of input variables and process parameters that have been demonstrated to provide assurance of product quality, i.e. that the product CQA's is met. The key characteristic of probabilistic design spaces is that they provide quantitative information on the assurance of quality, accounting for both the mean and the variance of uncertain process parameters and variables. No combination of mass challenge and wash length was found for either resin lot which had a probability of

1.0 for the historical variability experienced in the load material, i.e. that would guarantee the CQA is always met. However, the large size of regions where the probability < 0.95 meant that rarely would the process fail to meet its objectives if the operating condition was specific to the resin lot in use. The large difference between operating conditions that give $p > 0.95$ for each resin are somewhat surprising given the small difference between the adsorption isotherm parameters, but are due to the very challenging CQA constraint, combined with the mean and variance of the inlet composition and concentration.

When the design space must be eligible for all resin lots, then the probability of achieving the correct product form distribution in the elution peak should be high for both resin lots. Fig. 8 shows an overlay of the two resins' probabilistic design spaces. Critically, there was no operating region where the probability of both the low and high resin lots remained > 0.95, i.e. risk of batch failure $< 5\%$. Even at the optimum operating condition where the two curves intersect (e.g. mass challenge 2 mg/ml, wash length 4 CV), the probability only reaches 0.84. As a result, the operating parameter ranges available for manufacturing are small, and at best, 16% of batches are still predicted to fail product quality specifications. In addition, the product form distribution will vary within the full allowable range ($0.25 < B < 0.45$), which is undesirable when the objective is to produce a consistent product.

Selecting operating conditions that are eligible for all resin lots also means that high risk regions are selected, where deviations from usual inlet stream composition can result in further performance issues. For this case study, significant increases in process robustness can be made by adapting the design space based on the resin lot in use, rather than fixing the design space for all resin lots. In practice, this would involve varying the length of the wash length based on the resin lot in use. This adaptive approach significantly increases the size of potential operating regions, improves flexibility to variations in process inputs, provides a more consistent product composition, and enables operation further away from high risk regions. This conclusion, that adaptive operation can bring significant benefits is in agreement with literature (Gétaz et al., 2013a,2013b), and is a viable mode of operation under FDA Quality by Design guidance (ICH, 2008a).

The probabilistic design spaces presented are particularly useful as they provide a quantitative measure of the assurance of product quality, which either validates the robustness of potential operating regions, or indicates a need for process improvement. The stochastic methodology can be easily extended to identify the level of control required on uncertain parameters/variables to achieve adequate assurance of quality, by systematically reducing the variance of uncertain parameters, and measuring the quality response. Alternatively, when parameter variability is reduced due to improvements and optimization by process operators as experience is built over a process lifetime, the method can identify how operating ranges can be expanded to give greater flexibility to process operators during manufacturing.

For this case study, the data indicates that if the operating parameter ranges must be fixed for all resin lots, then process improvements are needed. Without process improvements, operating regions that provide assurance of product quality are small and are not robust. We now consider how decreasing variability in the product form inlet concentrations via increased control of upstream unit operations can improve the assurance of quality when using an operating region fixed for all resins. Better control was assumed to result in less variability, and therefore a reduced standard deviation. A detailed description of how this can be achieved in practice is beyond the scope of this work, but could include modifications to upstream processes such as optimizing the elution stage of preceding affinity chromatographic separations. In any case, the study is a useful exercise for illustrating how stochastic simulation and mechanistic models can be used not only for quantifying risk associated with uncertainty, but for exploring the relationship between parameter and CQA variance, a key consideration when validating quality assurance.

Fig. 9 shows box plots indicating predicted variability of the product CQA (percentage B in the elution peak) as a function of the variability in the product form inlet concentrations. The mass challenge was 2 mg/ml and wash length 4 CV, previously identified as one of the optimal operating points for a fixed design space. The standard deviations considered include: 0.01, 0.015, 0.02 and 0.024. The probability of meeting the CQA specification is indicated next to each box plot (e.g. $p = 0.998$). As expected, reducing feed stream uncertainty (i.e. going from 0.024 towards 0.01) results in a reduction in product CQA variability, which translates into increases in the probability of meeting quality specifications (i.e. for low resin, $p = 0.0895$ to $p = 0.998$). When this is completed for all operating conditions, the size of regions with $p > 0.95$ (i.e. $< 5\%$ failure) increases. Fig. 10A shows the region where $p > 0.95$
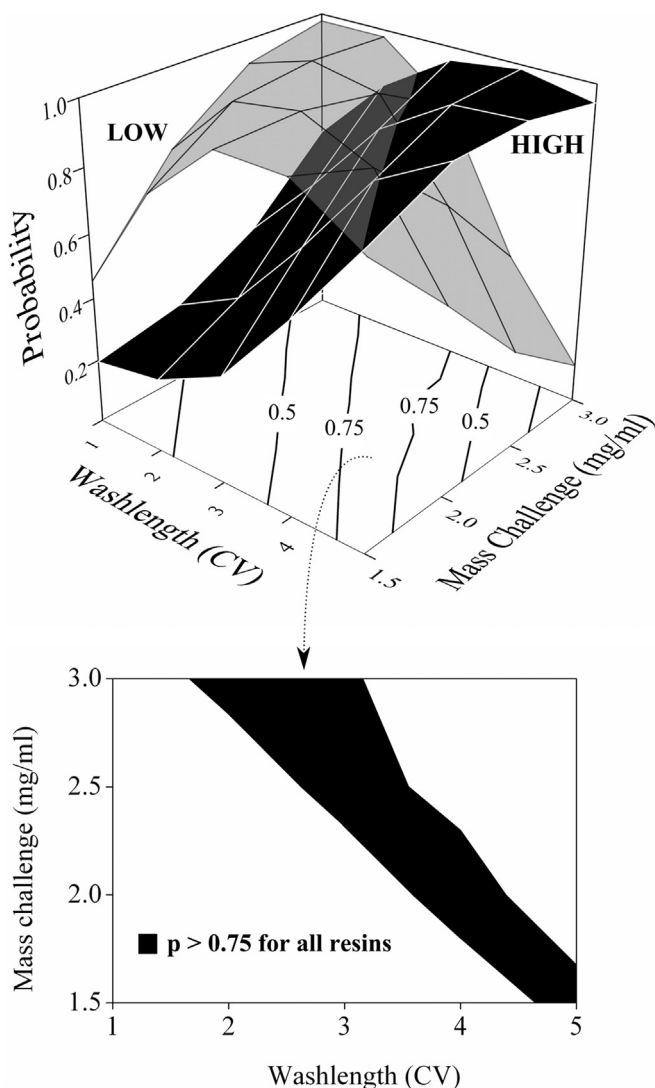

Fig. 8. Overlay of high and low resin probabilistic design spaces showing the operating parameter ranges where product quality is assured with $p > 0.75$ for all resins. No regions were found where product quality was assured with $p > 0.95$.
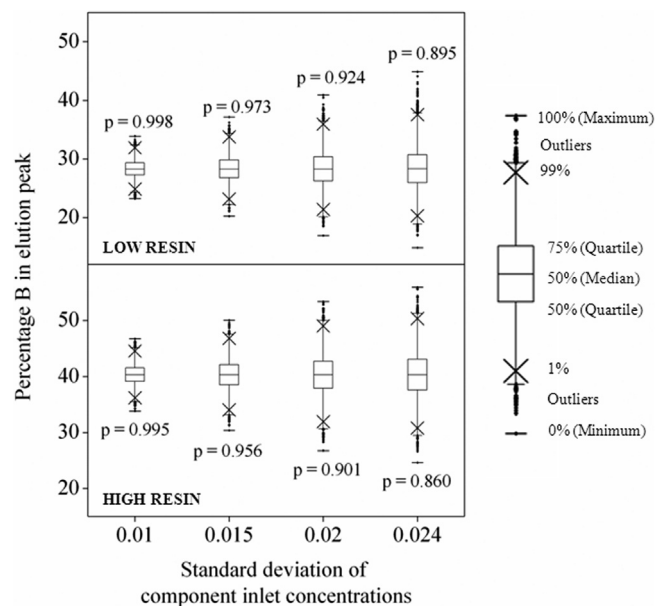

Fig. 9. Box plots showing variability of percentage B in elution peak as a function of variability in component inlet concentration, with probability of meeting quality specifications indicated next to each box plot, for a mass challenge of 2 mg/ml and wash length 4 CV.
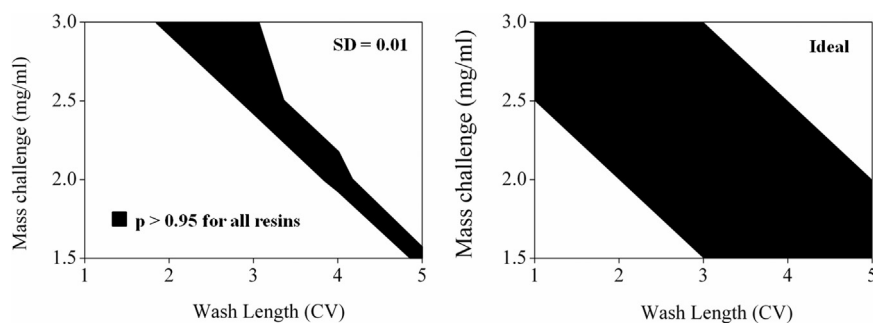
Fig. 10. Fixed design spaces. (left) Highest level of feed stream control considered in this work, SD=0.01. Area highlighted indicates probability of product quality assurance > 0.95. (right) Assuming no feed stream variability, and therefore the area highlighted shows $p=1.0$.

for both resins at the lowest inlet variability considered (SD=0.01). Even with this high level of control over the feed material, operating regions where p > 0.95 were significantly smaller than those available if the operating conditions were adapted according to the resin lot in use under normal inlet variability (Fig. 7). Fig. 10B shows the design space which assures product quality for all resins in an ideal (but unrealistic) system with no inlet variability. The large difference in size between Fig. 10A (ideal system with no inlet variability) and Fig. 10B (lowest inlet variability considered, SD=0.01), provides a stark demonstration of the importance of considering parameter variances when designing chromatography processes. If this is not accounted for, then the result may be unrealistically good expectations and in turn high failure rates.

5. Conclusion

In this paper, a model based approach was used to identify robust operating conditions for an industrial hydrophobic interaction chromatography where resin lot variability, combined with a variable feed stream, was resulting in serious performance issues during the purification of a multi component therapeutic protein from crude feed material. FDA guidance encourages the application of mechanistic models to improve process understanding, based on fundamental knowledge of the underlying causes which are linking process parameters to product CQA's. The methodology demonstrates how useful mechanistic models linked with stochastic simulation can be for this task, for as well as determining the functional relationship between process parameter values and the resulting value of the CQA, the use of models can quickly and efficiently determine the relationship between process parameter and CQA variances, a key aspect of providing assurance of product quality. This was not possible for the HIC in this case study using a design of experiment type of approach due to the impractical amount of resources that would be required.

The model based approach combines mechanistic models and stochastic simulation, and in this work is used to predict a key product CQA as function of mass challenge and wash length for polar extreme resin lots, designated high and low binding resin, whilst also accounting for uncertainty in feed stream composition and concentration. With normal process variability, no operating condition was found where the probability of both the low and high resin lots meeting product quality specifications remained > 0.95. The risk of batch failure when operating at the most favorable conditions found in this work was 16%, and selecting operating conditions that were eligible for both resin lots meant that operating conditions were not robust. Increasing control on the inlet concentration and composition was predicted to improve fixed design space robustness, but we found that using an adaptive

design space, where operating conditions are changed according to which resin lot is in use, was the favorable option.

Nomenclature

C^m	Mobile phase concentration (mg/ml)
C^{sp}	Stationary phase concentration (mg/ml)
C_{equil}	Concentration of the equilibration supernatant (mg/ml)
$C_{elution}$	Concentration of the elution supernatant (mg/ml)
CF	Compression factor
D_A	Apparent axial dispersion coefficient (cm^2/s)
F	Mobile phase flowrate (ml/s)
i	Component identifier
k_a	Equilibrium constant
L	Column length (cm)
M_t	Total amount of protein added to the micro well (mg)
N_C	Number of components
N_p	Number of theoretical plates
P_i^{load}	Component percentage in load material
P_i^m	Component percentage in equilibration supernatant
q_s	Saturation capacity (mg/ml)
q	Settled resin concentration (mg/ml)
t_0	Retention time (1/s)
t	Time (s)
u	Interstitial velocity (cm/s)
$V_{elution}$	Volume of the equilibration supernatant (ml)
V_{equil}	Volume of the elution supernatant (ml)
V_{resin}	Settled resin volume in microwell (ml)
V_C	Column volume (ml)
ϵ_T	Total column porosity

References

Borg, N., Westerberg, K., Andersson, N., von Lieres, E., Nilsson, N., 2013. Effects of uncertainties in experimental conditions on the estimation of adsorption model parameters in preparative chromatography. Comput. Chem. Eng. 55, 148–157.

Brooks, C.A., Cramer, S.M., 1992. Steric mass-action ion exchange: displacement profiles and induced salt gradients. AIChE J. 38, 1969–1978.

Close, E.J., Salm, J.R., Bracewell, D.G., Sorensen, E., 2014. Modelling of industrial biopharmaceutical multicomponent chromatography. Chem. Eng. Res. Des., http://dx.doi.org/10.1016/j.cherd.2013.10.022, in press

Coffman, J.L., Kramarczyk, J.F., Kelley, B.D., 2008. High–throughput screening of chromatographic seperations: 1. Method development and column modeling. Biotechnol. Bioeng. 100, 605–618.

Degerman, M., Jakobsson, N., Nilsson, B., 2007. Modeling and optimization of preperative reversed – phase liquid chromatography for insulin purification. J. Chromatogr. A. 1162, 41–49.

Degerman, M., Westerberg, K., Nilsson, N., 2009. A Determining critical process parameters and process robustness in preparative chromatography – a model based approach. Chem. Eng. Technol. 32, 903–911.

Gerontas, S., Asplund, M., Hjorth, R., Bracewell, D.G., 2010. Integration of scale – down experimentation and general rate modelling to predict manufacturing scale chromatographic seperations. J. Chromatogr. A. 1217, 6917–6926.

Gétaz, D., Stroehleina, G., Butté, A., Morbidelli, 2013a. Model-based design of peptide chromatographic purification processes. J. Chromatogr. A. 1284, 69–79.

Gétaz, D., Butté, A., Morbidelli, 2013b. Model-based design space determination of peptide chromatographic purification processes. J. Chromatogr. A 1284, 80–87.

Guiochon, G., Goldshan-Shirazi, S., Katti, A.M., 1994. Fundamentals of Preperative and Non-linear Chromatography. Academic Press, Boston.

Harms, J., Wang, X., Kim, T., Yang, X., Rathore, A.S., 2008. Defining process design space for biotech products: case study of pichia pastoris fermentation. Biotechnol. Prog. 24, 655–662.

International Conference of Harmonisation (2005). ICH Harmonised Tripartite Guideline: Q9 Quality Risk Management.

International Conference of Harmonisation (2008a). ICH Harmonised Tripartite Guideline: Q8 Pharmaceutical Development.

International Conference of Harmonisation (2008b). ICH Harmonised Tripartite Guideline: Q10 Pharmaceutical Quality Systems.

Jakobsson, N., Degerman, M., Nilsson, B., 2005. Optimization and robustness analysis of a hydrophobic interaction chromatography step. J. Chromatogr. A 1063, 99–109.

Jiang, C., Flansburg, L., Ghose, S., Jorjorian, P., Shukla, A., 2010. Defining process design space for a hydrophobic interaction chromatography (HIC) purification step: Application of quality by design (QbD) principles. Biotechnol. Bioeng. 107, 985–997.

Kaczmarski, K., Antos, D., Sajonz, H., Sajonz, P., Guiochon, G., 2001. Comparitive modeling of breakthrough curves of bovine serum albumin in anion – exchange chromatography. J. Chromatogr. A 925, 1–17.

McCue, J.T., Engel, P., Ng, A., Macniven, R., Thommes, J., 2008. Modeling of protein/ aggregate purification and separation using hydrophobic interaction chromatography. Bioprocess. Biosyst. Eng. 31, 261–275.

McCue, J.T., Cecchini, D., Chu, C., Liu, W., Spann, A., 2007. Application of a two – dimensional model for predicting the pressure – flow and compression properties during column packing scale – up. J. Chromatogr. A 1145, 89–101.

Melter, L., Butte, A., Morbidelli, M., 2008. Preperative weak cation – exchange chromatography of monoclonal antibody variants: 1. Single component adsorption. J. Chromatogr. A 1200, 156–165.

Mollerup, J.M., Hansen, T.B., Kidal, S., Sejergaard, L., Hansen, E., Staby, A., 2007. Development, modelling, optimization and scale – up of chromatographic purification of a therapeutic protein. Fluid Phase Equilib. 261, 133–139.

Mollerup, J.M., 2008. A review of the thermodynamics of protein association to ligands, protein adsorption, and adsorption isotherms. Chem. Eng. Technol. 31, 864–874.

Nagrath, D., Xia, F., Cramer, S.M., 2011. Characterization and modeling of nonlinear hydrophobic interaction chromatographic systems. J. Chromatogr. A. 1218, 1219–1226.

Nfor, B.K., Ahamed, T., van Dedem, G.W.K., Verhaert, PDEM, van der Wielen, L.A.M., Eppink, L.H.M., de Sandt, E.J.A.X., Ottens, M., 2013. Model-based rational methodology for protein purification process synthesis. Chem. Eng. Sci. 89, 185–195.

Ng, C.K.S., Osuna-Sanchez, H., Valery, E., Sørensen, E., Bracewell, D.G., 2012. Design of high productivity antibody capture by protein A chromatography using an integrated experimental and modeling approach. J Chromatogr. B 899, 116–126.

Osberghaus, A., Drechsel, K., Hansen, S., Hepbildikler, S.K., Nath, S., Haindl, M., vonLieres, E., Hubbuch, J., 2012. Model – integrated process development demonstrated on the optimization of a robotic cation exchange step. Chem. Eng. Sci. 76, 129–139.

Process Systems Enterprise, 2013. gPROMS, ⟨www.psenterprise.com/gproms⟩.

Rathore, A.S., Winkle, H., 2009. Quality by design for pharmaceuticals: regulatory perspective and approach. Nat. Biotechnol. 27, 26–34.

Rathore, A.S., 2009. Roadmap for implementation of quality by design (QbD) for Biotechnology products. Trends Biotechnol. 27, 546–555.

Seidel-Morgenstern, A., 2004. Review: experimental determination of single solute and competitive adsorption isotherms. J. Chromatogr. A 1037, 255–272.

Westerberg, K., Hansen, E.B., Degerman, D., Hansen, T.B., Nilsson, B., 2012. Model-based process challenge of an industrial ion-exchange chromatography step. Chem. Eng. Technol. 35, 183–190.